Mass Spectrometry & Purification Techniques

Chahboune and Sarakha, Mass Spectrom Purif Tech 2018, 4:1
DOI: 10.4172/2469-9861.1000125

Research Article Open Access

Homolytic Scission as the Main Pathway in the Liquid Chromatography/ Electrospray Ionization Quadrupole Time-of-Flight Mass Spectrometry of Mesotrione and its Photoproducts

Rajae Chahboune and Mohamed Sarakha*

CNRS, SIGMA Clermont, Clermont-Ferrand Institute of Chemistry, Clermont Auvergne University, F-63000, Clermont-Ferrand, France

Abstract

The indirect photochemical degradation of mesotrione induced by humic substances was studied by excitation with a solar light simulator. The disappearance rate constant increased by increasing the concentration of molecular oxygen. Three main byproducts were observed. They all arise from the dissociation of the non- aromatic cycle. Collision-induced dissociation tandem mass spectrometry (CID-MS/MS) of the deprotonated molecule was carried out and the effect of the collision energy as well as the elemental compositions of the products ions was used to propose the chemical structures. The presence in the chemical structure of the SO2-Me moiety permitted several types of homolytic scissions leading to the formation of radical anions.

Keywords: Mesotrione; Humic substances; Homolytic scission; ESI/MS/MS; Hydroxyl radical

Introduction

Nowadays, great concern deals with the effect of the contamination of groundwater and surface water owing to the extensive use of pesticides for agricultural purposes. Of course they play a beneficial role in agriculture, however, they have been largely described as causing important environmental problems. Thus, the extensive use of pesticides and therefore the contamination of air, soil, surface and ground waters has an unavoidable effect of human health.

Mesotrione [2-(4-methylsulfonyl-2-nitrobenzoyl)-1,3-cyclohexanedione] is a pesticide that belongs to a new class of triketone herbicides [1]. It is widely used for pre as well as post-emergence broadleaved weed control in corn. It is supposed to act by competitive inhibition of the enzyme 4-hydroxyphenylpyruvate dioxygenase (HPPD) [2,3]. The fate of mesotrione under various environmental conditions has been the subject of several research activities [4-8]. As examples:

- Two different and main metabolites were identified in soils and plant and mammal metabolisms, namely MNBA (4-(methylsulfonyl)-2-nitrobenzoic acid) and AMBA (4-(methylsulfonyl)-2-aminobenzoic acid) [9] (Scheme 1).
- The direct excitation upon 365 nm leads to the disappearance of mesotrione [10]. This study clearly demonstrates that mesotrione sensitizes its own oxidation by involving the triplet excited state. This proceeds through singlet oxygen formation and sensitizes the oxidation of H-donors through electron or H-atom transfer [10]. Besides MNBA, the photochemical degradation of mesotrione leads to the formation of two more byproducts arising from the scission of the non-aromatic cycle (Scheme 2).

Once mesotrione is in surface waters, it may undergo direct and/or indirect phototransformation. The direct phototransformation is observed when mesotrione absorbs itself the light while the indirect transformation is obtained when other substances absorb light and produce highly reactive species which can then react with mesotrione and induce its disappearance. Natural waters contain several species that may play the role of inducers such as nitrates, iron(III) species and of course dissolved organic matter DOM [11,12]. The latter substances are known to produce several kinds of reactive species such as: hydroxyl radicals, solvated electrons, reactive triplet excited states [13].

This paper deals with the photodegradation of mesotrione by commercial humic substances **HS**. It mainly concerns the analytical point of view of such photochemical point by the elucidation of the generated byproducts through their LC/MS/MS data. To our knowledge, no mechanisms of mesotrione and its byproducts electrospray fragmentation have been reported until no.

Experimental Section

Materials

Mesotrione, with a IUPAC name 2-[4-(Methylsulfonyl)-2-nitrobenzoyl]cyclohexane-1,3-dione (CAS number 104206-82-8), was obtained from Pestanal and was used as received. Humic substances (HS) were purchased Aldrich and used as received. Except when stated, all the other reagents were of the purest grade commercially available and were used without further purification. All the solutions were prepared with deionised ultrapure water that was purified with Milli-Q devise (Millipore) and its purity was controlled by its resistivity. pH measurements were carried out with a JENWAY 3310. For the irradiation with humic substances, the pH was adjusted to 6.5 with phosphates. The ionic strength was not controlled.

Irradiations setups

The Irradiation experiments using Humic substances (**HS**) were performed at 365 in an elliptical stainless steel cylinder. A high pressure mercury lamp (Philips HPW, 125 W) was located at a focal axis of the elliptical cylinder. An inner filter selected the emission at 365 nm permitting the selective excitation of Humic substances. The reactor (water-jacketed pyrex tube-diameter 2.8 cm) was centred at the other focal axis. The solution (roughly 30 ml) was continuously stirred with a magnetic bar during irradiation.

***Corresponding author:** Mohamed Sarakha, CNRS, SIGMA Clermont, Clermont-Ferrand Institute of Chemistry, Clermont Auvergne University, F-63000, Clermont-Ferrand, France, Tel: +33473407170; E-mail: mohamed.sarakha@uca.fr

Received April 06, 2018; **Accepted** April 09, 2018; **Published** April 16, 2018

Citation: Chahboune R, Sarakha M (2018) Homolytic Scission as the Main Pathway in the Liquid Chromatography/Electrospray Ionization Quadrupole Time-of-Flight Mass Spectrometry of Mesotrione and its Photoproducts. Mass Spectrom Purif Tech 4: 125. doi:10.4172/2469-9861.1000125

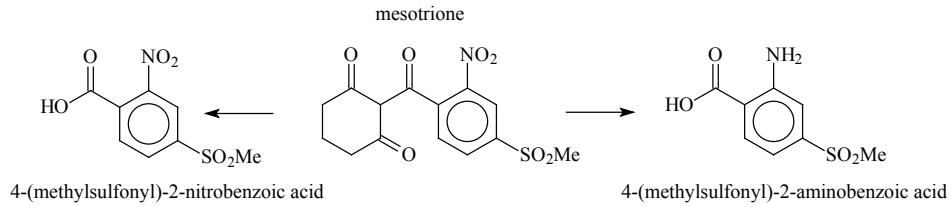

Scheme 1: Metabolites in soils and plant mammal metabolisms.

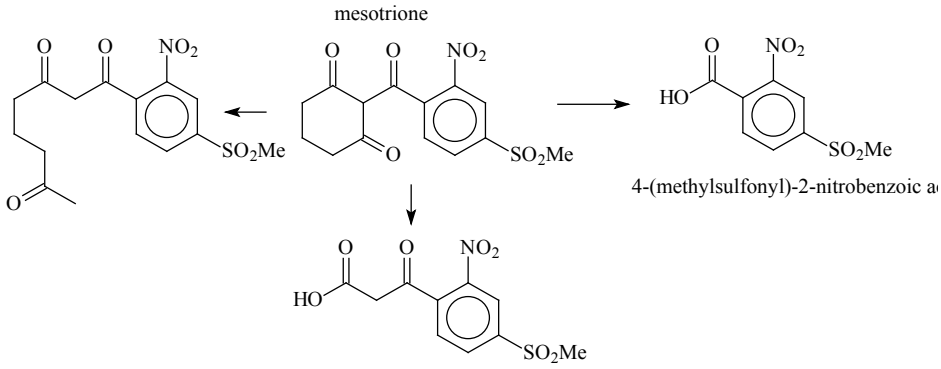

Scheme 2: Byproducts from photochemical degradation of mesotrione.

The irradiations were also performed using a solar light simulator. The prepared samples were irradiated horizontally in a Suntest CPS photoreactor (Atlas, Moussy le neuf, France) equipped with a xenon lamp and a filter that prevents the transmission of wavelength below 290 nm. The lamp was operated at an intensity of 750 W/m^2. The temperature of the sample was roughly maintained at 20 °C by a continuous flow of cold water through the bottom of the photoreactor.

For direct excitation of mesotrione, the irradiations were performed in a cylinder reactor made in stainless steel equipped with two germicidal lamps (Mazda T815 15W) emitting selectively at 254 nm and symmetrically installed around the cylinder. The reactor, a quartz tube (d=2.5 cm) containing a maximum of 25 mL solution, was located in the centre of the container.

Analytical and spectroscopic equipments

The direct as well as the induced photodegradation by humic substances of mesotrione and the formation of the by-products were followed by Waters Alliance 2695 (Waters SA, St-Quentin en Yvelines, France) photodiode array detector (DAD) chromatograph. A reversed-phase column distributed by Phenomenex (Kinetex MS C18, 2.6 µm, 100 mm × 2.1 mm) was used at a flow rate of 0.2 mL min^{-1} and the injected volume was 20 µL. The elution was accomplished, using an isocratic program, with water (0.1% formic acid) and acetonitrile at 75% and 25% respectively.

A Waters/Micromass LC/QTOF tandem mass spectrometer (Micromass, Manchester, UK), with an orthogonal geometry Z-spray ion source, was used for LC/ESI/MS and LC/ESI/MS^2 experiments. LC separation was performed using the gradient program reported in the literature. The degradation of Chloridazon and the formation of the by-products were followed by Waters Alliance 2695 (Waters SA, St-Quentin en Yvelines, France) photodiode array detector (DAD) chromatograph. A reversed-phase column distributed by Phenomenex (Kinetex MS C18, 2.6 µm, 100 mm × 2.1 mm) was used at a flow rate of 0.2 mL min^{-1} and the injected volume was 20 µL. The elution was accomplished, using an isocratic program, with water (0.1% formic acid) and acetonitrile at 60% and 40% respectively.

A Waters/Micromass LC/QTOF tandem mass spectrometer (Micromass, Manchester, UK), with an orthogonal geometry Z-spray ion source, was used for LC/ESI/MS and LC/ESI/MS^2 experiments. Eluate was subjected to electrospray ionization (ESI) in the positive as well as negative ion modes and resulted in the formation of protonated and deprotonated molecules of the sample components respectively. Scanning was performed in the range between m/z 60 and 600. The elemental composition of the recorded ions was further determined using MassLynx Elemental Composition software V4.1 (Micromass). The maximum deviation was set to 10 ppm, and C, H, N, O, Cl were selected as possible elements present. Five scans were combined before the integration of the individual peaks.

The desolvation and ion source temperatures were set at 250°C and 100°C, respectively. Nitrogen was used as the nebulizer (35 L/h) as well as a desolvation gas (350 L/h). The optimized voltages for the probe and ion source components (to produce maximum intensity) were 3 kV for the stainless-steel capillary, 35 V for the sample cone and 1 V for the extractor cone.

Tandem mass spectrometric (MS/MS) experiments in collisionally induced dissociation (CID) mode were performed using argon in the collision cell at a pressure of 4.0 × 10^{-3} mbar. A collision energy gradient (15-35 V) was used for preliminary fingerprints and specific energies were then used to unambiguously assign the product ions. The $[M+H]^+$ or $[M-H]^-$ precursor ions was used as a lock masses for the MS/MS experiments and allowed for accurate mass measurements to be undertaken. The ion formulae were determined by restricting the possible elements present to those in the precursor ion formulae, and setting the maximum allowed deviation in the mass measurements to 20 ppm.

Results and Discussion

The UV-visible absorption spectrum of mesotrione highly depends on the pH of the solution. At pH<3, it exhibits two absorption bands at 274 and 220 nm with a shoulder at roughly 230 nm. However, at higher pH values, a unique band is observed at 255 nm with a shoulder at 291 nm. Such behaviour is owing to a protolytic equilibrium that involves the proton at the α-position of the three ketones functions. The pKa is estimated 3.1 [10]. The anionic form presents several mesomeric forms owing to the presence of the three ketones site (Scheme 3).

Aerated solutions of mesotrione (1.0×10^{-4} mol L^{-1}) and Humic substances **HS** (0.15 g L^{-1}) buffered at pH=5.6 were illuminated by a solar light simulator (suntest photoreactor) under the conditions given in the experimental part. Under the irradiation wavelengths (λ>290 nm), the photons were mainly absorbed by **HS**. In the absence of **HS**, the conversion of mesotrione was estimated to less than 5% after about 5 hours of illumination. As observed in Figure 1, the conversion of mesotrione reached 60% within 7 hours irradiation time with a pseudo first order kinetics. The rate constant was estimated to 0.13 h^{-1}. When the irradiation was undertaken at 365 nm, the conversion was evaluated to about 19% after 7 hours owing to the low absorbance of **HS** at the excitation wavelength. The irradiation within the same conditions of the mixture mesotrione and **HS** (1.0×10^{-4} mol L^{-1}/ 0.15 g L^{-1}) at 254 nm leads to higher conversion percentage, roughly 90% after 4 hours irradiation time. It should be noted that at such wavelength, the photons were absorbed by both components, namely mesotrione and **HS**, and thus, the disappearance resulted from two pathways: direct phototransformation and transformation photoinduced by excitation of **HS**. In all cases, the degradation rate was much slower in oxygen free solutions, indicating that oxygen plays an important role in the photochemical behaviour of mesotrione.

Following irradiations and after a conversion of about 30% of mesotrione, three main byproducts were observed from the early stages of excitation (Figure 2). Their concentrations clearly increased as a function of irradiation time indicating their formation as primary products.

The three products **P1**, **P2** and **P3** were clearly detected by using HPLC equipped with a diode array detector at the retention times: 1.8; 3.3 and 8.2 minutes respectively when mesotrione was observed at 12.3 minutes. In order to identify the generated byproducts, HPLC/ESI/MS as well as HPLC/ESI/MS/ MS experiments were undertaken in both positive and negative modes. The first set of experiments permitted us to obtain the accurate mass and the molecular formulae and mass error values were obtained using the elemental composition tool in the MassLync V4.1 software. In the second set of experiments, namely MS^2 data, the $[M+H]^+$ (or $[M-H]^-$) accurate mass was used as a lock mass for the accurate mass determinations for the generated fragment ions.

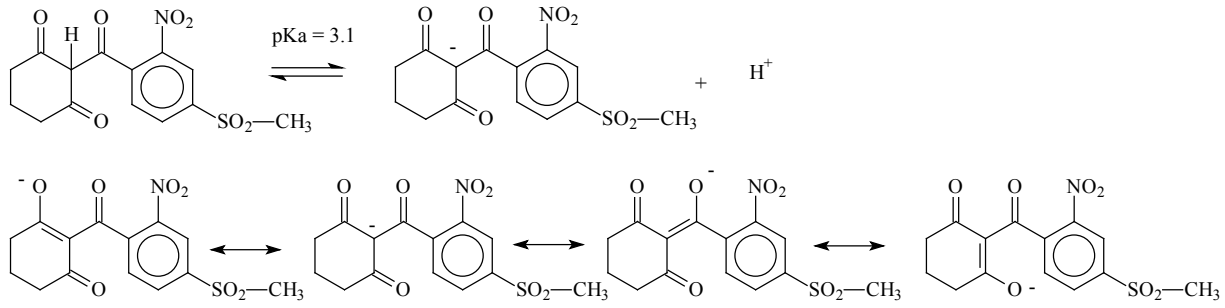

Scheme 3: Protolytic equilibrium of mesotrione and the various mesomeric forms.

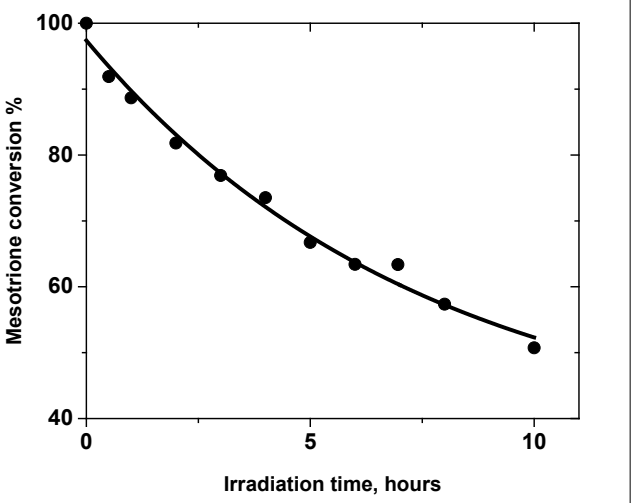

Figure 1: Kinetic profile for the degradation of mesotrione under illumination with a solar light simulator. Aerated Solutions of mesotrione (1.0×10^{-4} mol L^{-1}) and Humic substances **HS** (0.15 g L^{-1}) buffered at pH=5.6.

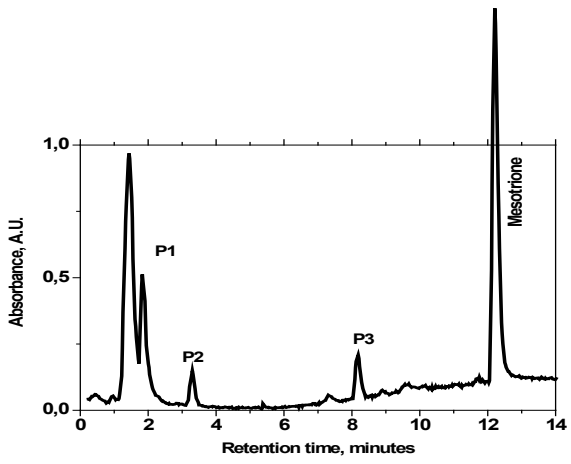

Figure 2: HPLC chromatogram of the irradiated solution of the mixture mesotrione/ Humic substances. Aerated Solutions of mesotrione (1.0×10^{-4} mol L^{-1}) and Humic substances **HS** (0.15 g L^{-1}) buffered at pH=5.6. Irradiation with a solar light simulator.

Table 1 gives the main results obtained by HPLC/ESI/MS. It shows It should be noted that mesotrione was easily detected in both positive and negative modes while the byproducts were mainly observed at relatively high intensities in negative mode. The reason why the results will be give inhere in the negative mode. As shown in Figure 3, under our experimental conditions, the ESI-/MS spectrum of mesotrione is dominated by two peaks of the ions m/z 338 and 291 (ions **1a**) corresponding to [mesotrione-H]$^-$ and to the ion corresponding to the elimination of HNO_2. This shows that even in soft conditions, the parent ion easily decomposes with the formation of the ion **1a** (referring to the text below). The accurate obtained mass of the deprotonated form of mesotrione (333.0332) is in perfect agreement with the elemental composition $C_{14}H_{12}NO_7S^-$ (mass error -0.7 ppm).

By close analyses of the elemental compositions we can conclude that the three formed byproducts present seven atoms of carbon which clearly indicates the loss of a part of mesotrione. Moreover, all the products contain the sulphur atom while one of them, namely **P2**, appears without the nitrogen atom.

In order to have useful information for the precise identification of the unknown generates, the fragmentation of the parent compound mesotrione was carefully studied.

Mass spectra analyses of the parent compound mesotrione

Figure 4 represents the CID spectrum of [mesotrione-H$^+$]$^-$ as obtained with a collision energy of 25 eV. It shows the presence of three major fragments ions: m/z 291 (**1a**), 249 (**1b**) and 212 (**1c**). Moreover, several minor ions are also obtained at m/z 276 (**1d**) 263 (**1e**), 227 (**1f**) and 184 (**1g**). All the data relative to these fragment ions are listed in Table 2.

The evolution of the intensities of the ions as a function of the collision energy clearly shows that the fragment ion **1a** (m/z=291) is formed in a primary step. This was observed even in soft MS conditions as specified above. It should be noted that all the other fragments are more likely arising from **1a** since their formations were only seen at collision energies higher than 15 eV.

The fragment ion **1a** with the elemental composition $C_{14}H_{11}O_5S^-$ (error+2.3 ppm) corresponds to the elimination of nitrous acid (HNO_2) as shown in Scheme 4. This proceeds through a cyclisation process and a transfer of hydrogen atom.

Once generated, the fragment ion **1a** (m/z=291) may be involved in various secondary degradation pathways leading to the formation of the other fragment ions. These pathways are gathered in Scheme 4 and presented as follows:

- An intramolecular elimination of carbon monoxide leading to the formation of **1e** (m/z 263; $C_{13}H_{11}O_4S^-$; -1,2 ppm) that presents a furan structure. Such fragment further eliminates the radical $^{\cdot}SO_2Me$ via a homolytic dissociation of the C-S bond that permits the generation the radical anion **1g** (m/z=184; $C_{12}H_8O_2^{\cdot-}$; error=-6.7 ppm).
- A homolytic dissociation of the S-methyl bond leading to the loss of the methyl radical and the formation of the fragment radical ion **1d** (m/z=276; $C_{13}H_8O_5S^{\cdot-}$; error+6.4 ppm). The latter fragment

m/z	Products	Retention time, min	Accurate mass	Calculated mass	Elemental composition	Error (ppm)
338	**Mesotrione**	12.2	338.0332	338.0334	$C_{14}H_{12}NO_7S^-$	-0.7
244	**P3**	8.2	243.9901	243.9916	$C_8H_6NO_6S^-$	-3.2
214	**P1**	1.8	214.0160	214.0174	$C_8H_8NO_4S^-$	-6.6
215	**P2**	3.3	215.0001	215.0014	$C_8H_7O_5S^-$	-6.1

Table 1: Data obtained from the HPLS/ESI-/MS.

Fragment ion	m/z	Accurate mass	Calculated mass	Elemental composition	Error (ppm)
1a	291	291.0334	291.0327	$C_{14}H_{11}O_5S^-$	+2.3
1d	276	276.0110	276.0092	$C_{13}H_8O_5S^{\cdot-}$	+6.4
1e	263	263.0375	263.0378	$C_{13}H_{11}O_4S^-$	-1.2
1b	249	249.0198	249.0222	$C_{12}H_9O_4S^-$	-9.5
1f	227	227.0692	227.0708	$C_{14}H_{11}O_3^-$	-7.1
1c	212	212.0497	212.0473	$C_{13}H_8O_3^{\cdot-}$	+11.1
1g	184	184.0512	184.0524	$C_{12}H_8O_2^{\cdot-}$	-6.7

Table 2: Accurate and exact masses and elemental composition of the fragment ions of [mesotrione-H$^+$]$^-$ as obtained with a collision energy of 25 eV.

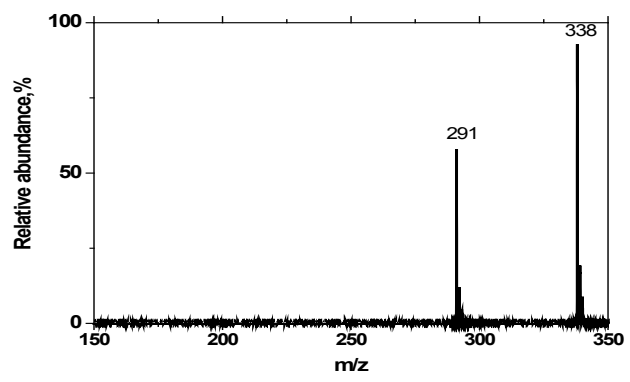

Figure 3: LC/ESI- spectrum of mesotrione.

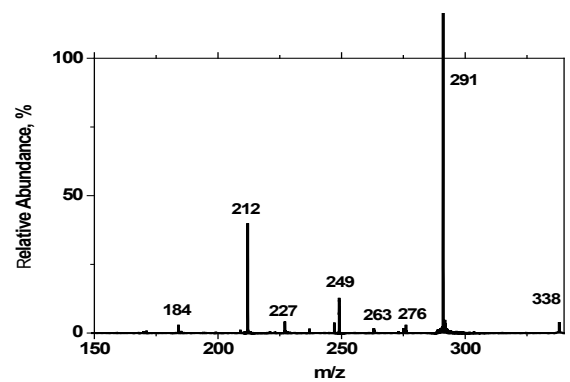

Figure 4: Collisional induced dissociation (DIC) spectrum of [mesotrione-H$^+$]$^-$ obtained at a collision energy of 25 eV.

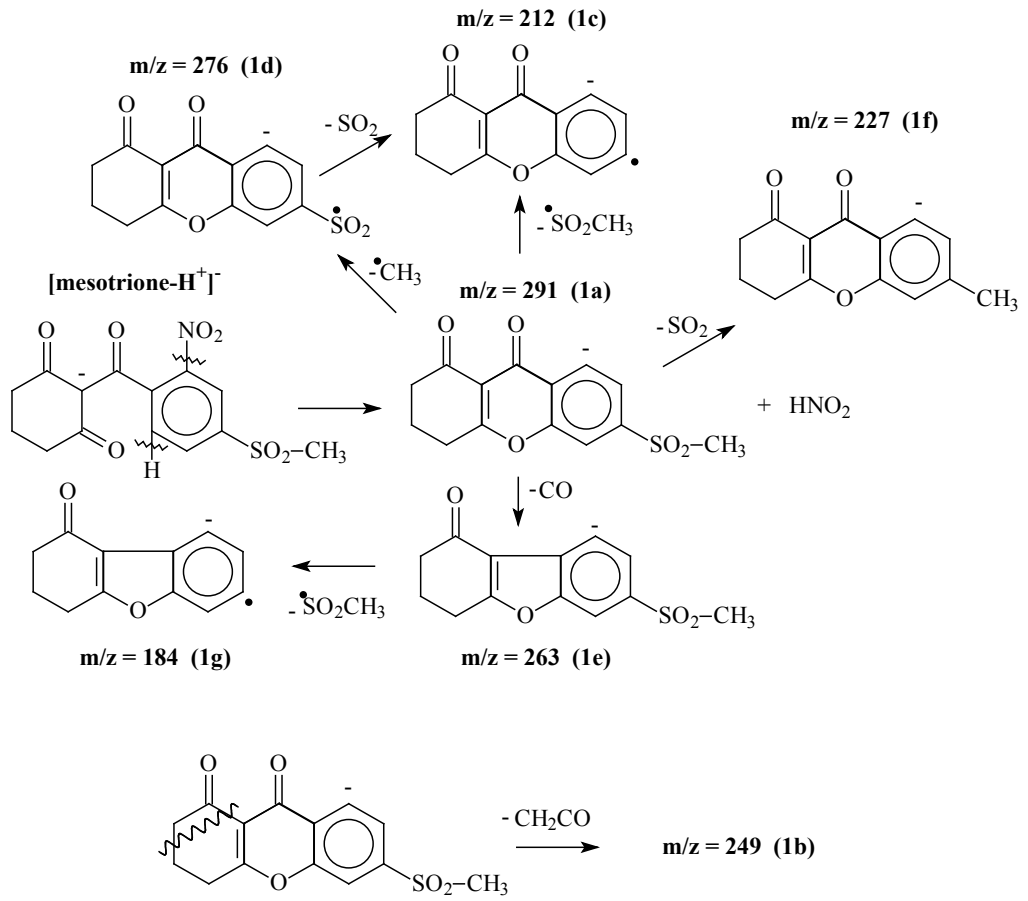

Scheme 4: Fragmentation pathways of [mesotrione-H$^+$]$^-$.

may lose in its turn a neutral molecule of sulfur dioxide to form **1c** (m/z=212; $C_{13}H_8O_3^-$).

- A homolytic scission of C-sulfur bond that correspond to an alternative second pathway for the formation of the fragment radical anion **1c** (m/z=212; $C_{13}H_8O_3^-$).
- The formation of the fragment **1f (m/z=227;** $C_{14}H_{11}O_3^-$) via an intramolecular sulphur dioxide elimination of SO_2.
- The formation of m/z=149 (**1b;** $C_{12}H_8O_2^-$) after the elimination of the neutral ketene structure CH_2CO.

As clearly shown above, homolytic scissions are largely presented as a guideline for the interpretation and elucidation of several fragment ions. These mainly involve the SO_2-CH_3 moiety.

Mass spectra analyses of the byproducts P1, P2 and P3

The two byproducts **P1** and **P3** that elutes at the retention time of 1.8 and 8.2 minutes respectively have elemental compositions that are different from each other ($C_8H_8NO_4S^-$ and $C_8H_6NO_6S^-$ respectively) by the number of hydrogen and oxygen. **P2** which has a retention time of 3.3 minutes and $C_8H_7O_5S^-$ as elemental composition lost the nitrogen atom. These products were already presented in the literature [2-4] and they correspond to the following structures (Scheme 5).

As for the parent compound mesotrione, their fragmentations pathways were studied in order to establish a general scheme for the fragmentation of compounds that present SO_2-CH_3 as a chemical moiety. The LC/ESI/MS/MS of **P1** is given in Figure 5 and the main data extracted.

As clearly shown in Table 3, despite the difference in the elemental compositions, the patterns of the ESI fragmentation for **P1** and **P2** are more likely the same. As for the parent compound, the generated fragment ions are similar with one unit of mass difference indicating the same chemical squeleton except for the fragment ion m/z=79 that is common to both products. However, **P3** presents only one main fragment ion corresponding the decarboxylation process. The fragmentation pathway of **P1** is presented in Scheme 6 and the same scheme may be taken for **P2** by replacing the NH_2 group by a OH group. As for mesotrione, the fragmentation proceeds through several homolytic scission involving SO_2-CH_3.

From the photochemical point of view, the formation of **P3** arises from the scission of non-aromatic moiety. This proceeds through the oxidation of mesotrione via direct oxidation or/and photosensitized by Humic substances (**HS**). The latter compounds are known to produce very reactive species such as hydroxyl radical or triplet excited states that are able to oxidize organic compounds. The formation of **P2** is owing to the oxidation of **P3** by the generated hydroxyl radical. **P1**

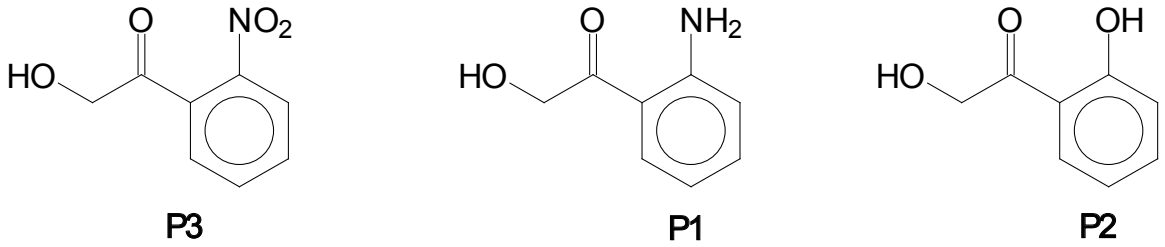

Scheme 5: Chemical structures for P1, P2 and P3.

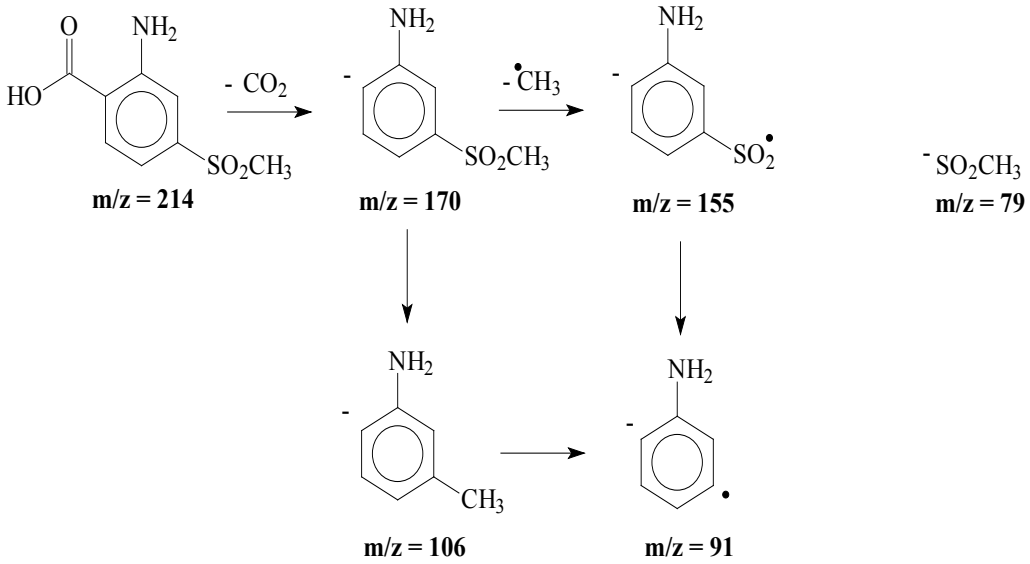

Scheme 6: ESI/MS/MS fragmentation pathways of **P1**.

P1 $C_8H_8NO_4S^-$ (m/z=214)				
m/z	**Accurate mass**	**Calculated mass**	**Elemental composition**	**Error (ppm)**
170	170.0283	170.0276	$C_7H_8NO_2S^-$	+4.3
155	155.0049	155.0041	$C_6H_5NO_2S^-$	+5.2
106	106.0642	106.0657	$C_7H_8N^-$	-13.9
91	91.0410	91.0422	$C_6H_5N^-$	-13.2
79	78.9862	78.9854	$SO_2CH_3^-$	+10.4
P2 $C_8H_7O_5S^-$ (m/z=215)				
171	171.0108	171.0116	$C_7H_7O_3S^-$	-4.6
156	155.9870	155.9881	$C_6H_4O_3S^-$	-7.2
107	107.0480	107.0497	$C_7H_7O^-$	-15.8
92	92.0273	92.0262	$C_6H_4O^-$	+11.8
79	78.9850	78.9854	$SO_2CH_3^-$	-4.8
P3 $C_8H_6NO_6S^-$ (m/z=244) The spectrum is dominated by the fragment ion at m/z=200 corresponding to the loss of carbon dioxide				

Table 3: Accurate and exact masses and elemental composition of the fragment ions of the byproducts **P1**, **P2** and **P3** as obtained with a collision energy of 25 eV.

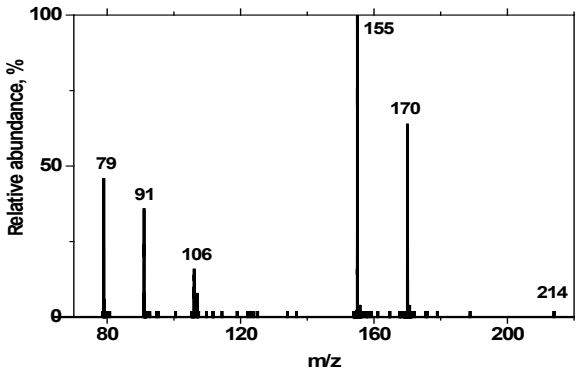

Figure 5: Collisional induced dissociation (DIC) spectrum of P1 obtained at a collision energy of 25 eV.

is clearly formed via a reduction process. This is only observed in the presence of Humic substance (**HS**) and may be due to the formation of solvated electron from the excitation of HS.

Conclusion

The LC/MS fragmentation of mesotrione and its byproducts allows for unequivocal elucidation of the chemical structures during the photosensitized degradation of mesotrione with humic substances **HS**. Such degradation involves first the scission of the non-aromatic moiety leading to the formation of a carboxylic form (product **P3**) and second the oxidation of the generated compound by the hydroxyl radicals. It also involves, a reduction process via the formation of solvated electron from Humic substances.

The presence in the chemical structure of the SO_2-CH_3 group permitted the observation in LC/ESI/MS/MS fragmentation of mesotrione, **P1** and **P2** of various homolytic bond scissions via the dissociation of C-S and S-CH_3 bonds.

Acknowledgements

The authors would like to thank Martin Leremboure for his important help with the LC/ESI/MS experiments.

References

1. Mitchell G, Bartlett DW, Fraser TEM, Hawkes TR, Holt DC, et al. (2001) Mesotrione: A new selective herbicide for use in maize. Pest Manage Sci 57: 120-128.
2. Rouchaud J, Neus O, Cools K, Bulcke R (2000) Dissipation of the triketone mesotrione herbicide in the soil of corn crops grown on different soil types. Toxicol Environ Chem 77: 31-40.
3. Beaudegnies R, Edmunds AJF, Fraser TEM, Hall RG, Hawkes TR, et al. (2009) Herbicidal 4-hydroxyphenylpyruvate dioxygenase inhibitors - a review of the triketone chemistry story from a Syngenta perspective. Bioorg Med Chem 17: 4134-4152.
4. Person AL, Siampiringue M, Sarakha M, Moncomble A, Cornard JP (2016) J Photochem Photobiol A: Chem 315: 76-81.
5. Bensalah N, Khodary A, Abdel-Wohab A (2011) Kinetic and mechanistic investigations of mesotrione degradation in aqueous medium by Fenton process. J Hazad Mat 189: 479-485.
6. Wang C, Harwood JD, Zhang Q (2018) Oxidative stress and DNA damage in common carp (Cyprinus carpio) exposed to the herbicide mesotrione. Chemosphere 193: 1080-1086.
7. Durand S, Sancelme M, Besse-Hoggan P, Combourieu B (2010) Biodegradation pathway of mesotrione: complementarities of NMR, LC-NMR and LC-MS for qualitative and quantitative metabolic profiling. Chemosphere 81: 372-380.
8. Krajczewska K, Maj J (2016) Degradation study of mesotrione and other triketone herbicides on soils and sediments. J Soils Sediments 16: 125-133.
9. Alferness P, Wiebe L (2002) Determination of mesotrione residues and metabolites in crops, soil, and water by liquid chromatography with fluorescence detection. J Agric Food Chem 50: 3926-3934.
10. Hall AT, Richard C (2006) Simulated solar light irradiation of mesotrione in natural waters. Environ Sci Technol 40: 3842-3847.
11. Boule P, Bolte M, Richard C (1999) Phototransformations Induced in Aquatic Media by NO3-/NO2, FeIII and Humic Substances. Handbook Environ Chem 2: 181-215.
12. Zepp RG, Baughman GL, Schlotzhauer PF (1981) Comparison of photochemical behavior of various humic substances in water: II. Photosensitized oxygenations. Chemosphere 10: 109-117.
13. Canonica S, Hellrung B (2000) Oxidation of phenols by triplet aromatic ketones in aqueous solution. J Phys Chem A 104: 1226-1232.